JOURNAL OF MATERIALS SCIENCE 30 (1995) 6281–6287

Silica fracture

Part III *Five- and six-fold ring contraction models*

J. K. WEST, L. L. HENCH
Advanced Materials Research Center, University of Florida, Alachua, FL 32615, USA

In part I of this series, a ring contraction model was proposed as the basic mechanism of slow crack growth in silica glass. AM1 molecular orbital theory running on a CAChe workstation was used to find the transition state for the contraction of a 4-fold ring into a 3-fold ring. Using the same AM1 method, the predicted transition state has been found for the contraction of a 5-fold ring into a 4-fold ring. The activation barrier to fracture for this contraction is $E_f = +7.9$ Kcal mol^{-1} using Unrestricted Hartree Fock (UHF) theory. As would be expected, the barrier calculated for Restricted Hartree Fock (RHF) was a little higher at $E_f = +14.8$ Kcal mol^{-1}. This confirms our initial hypothesis that ring contraction can lead to much lower fracture energies than expected from simple Si–O bond breaking. Several different schemes of ring contractions are possible for both 5-fold and 6-fold ring structures. All contraction paths have different intermediate structures that lead to the same end point of slow crack growth. The various barriers to fracture range from +8 to +52 Kcal mol^{-1} for the 5-fold ring contractions and from +9 to +41 Kcal mol^{-1} for 6-fold ring contractions.

1. Introduction

In parts I and II of this series, both the water-free fracture [1] and fracture due to hydrolysis of amorphous silica [2] (a-silica) were modelled at the atomic level using AM1 semi-empirical molecular orbital theory [3–5]. It was predicted that slow crack growth is related to the size of ring structures (within a-silica) encountered by the crack tip. The crack tip supplies energy to the rings of silica tetrahedra and is guided toward the lowest possible barrier to fracture by the distribution of ring sizes it encounters. If the crack tip intersects a 4-fold (D_1) silica ring, the fracture barrier via ring contraction is large; i.e. +65 Kcal mol^{-1}, as shown in Fig. 1. This value is still significantly lower than the 96 Kcal mol^{-1} barrier to fracture an Si–O bond in a 3-fold (D_2) ring [1] and is due to the formation of metastable pentacoordinated silicon in the transition state [6–8]. Fig. 1 also shows a prediction that fracture via ring contractions should also be possible for 5-fold and 6-fold silica rings. In this study, 5- and 6-fold rings were strained to produce ring contraction and eventual Si–O–Si bond breakage. It was discovered that several different reaction pathways are available in these larger rings for fracture to occur.

Our earlier study showed that when water is present silica rings open more easily as the ring size decreases [2]. This effect of water-enhanced ring-hydrolysis interchanges the relative energy required for breaking of 4-fold and 3-fold rings. A 4-fold ring is more stable than a 3-fold ring with respect to hydrolysis but is "less" stable with respect to water-free fracture via ring contraction. Thus, as water interacts with S–O–Si bonds at the tip of a fracture the interactions favoured will be the lowest energy path for hydrolysis. The crack front will tend to follow a path that optimizes the number of 3-fold rings encountered. Only if there is a local region where the pathway between 3-fold rings is too long will the crack front be arrested by the higher energy of hydrolysis of 4-fold rings. Applying increments in stress (increasing K) will enlarge the strain field and increase the probability that a water molecule in the crack tip will encounter a 3-fold ring. Thus, a dependence of crack velocity on stress intensity will occur in a humid environment, as shown in Region I of the V–K curve in Fig. 2 [2, 9–11]. In vacuum, the crack tip will tend to follow the 4-fold rings in a quantized, step-like manner to pursue the lowest energy path through the structure.

The crack velocity (V) versus stress intensity (K_1) relationship for silicate glasses, established by Weiderhorn [11], is shown in Fig. 2. These curves can be classically reproduced by a rate equation of the form:

$$V = V_0 \exp\left[\frac{(-E_a + \beta K_1)}{RT}\right] \quad (1)$$

where E_a is the activation energy for ring size a; β is a constant, R = gas constant, T is the temperature, V_0 is some initial crack velocity. The term $(-E_a + \beta K_1)$ is the energy term that characterizes the energy of fracture. This equation can be rearranged by taking the natural log of both sides:

$$\ln V = \left(\frac{\beta}{RT}\right)K_1 + \left(\frac{\ln V_0 - E_a}{RT}\right) \quad (2)$$

0022–2461

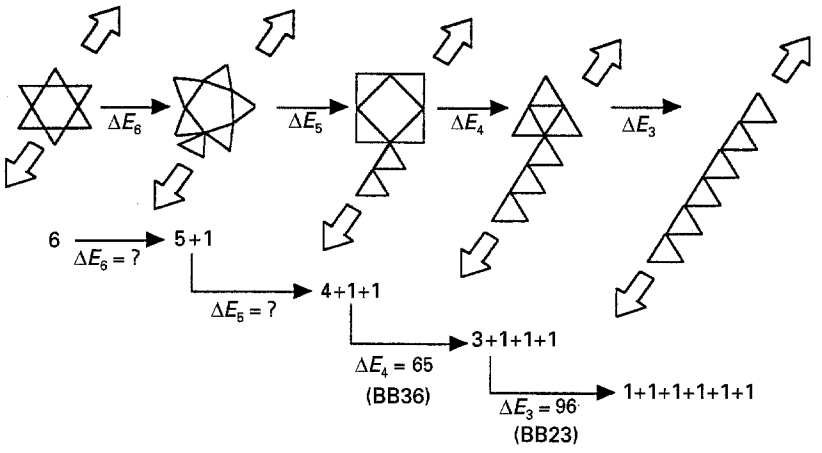

Figure 1 Ring contraction scheme during a-silica fracture.

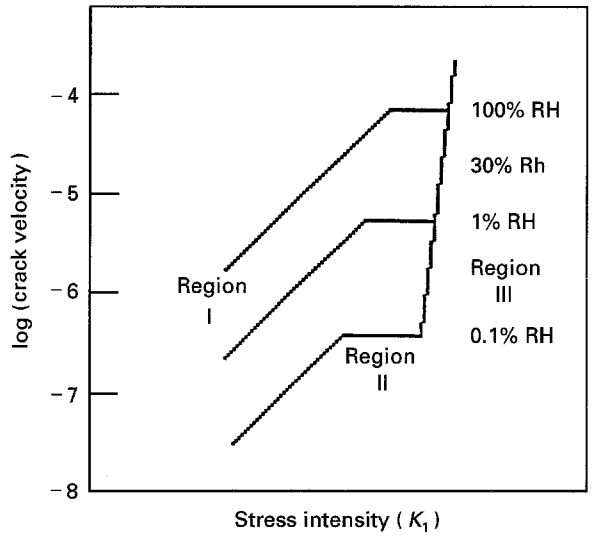

Figure 2 Velocity versus stress intensity (V–K) curve for slow crack growth in silica. Region I – hydrolysis controlled; Region II – diffusion controlled; Region III – ring contraction controlled.

Therefore, the slope, β/RT, should remain constant for different kinds of barriers, E_a. However, if the concentration of the different kind of barriers is different, then β should be directly proportional to the concentration of the ring structures that make up the various barriers:

$$\beta \propto [\text{ring structures}] \tag{3}$$

Therefore, there should be a series of terms that make up a quantized structural model for slow crack velocity based on ring size and ring concentrations: where N is the largest ring size in the bulk material.

$$\ln V = \sum_{a=2}^{N} \left[\left(\frac{\beta_a}{RT} \right) K_1 + \left(\ln V_0 - \frac{E_a}{RT} \right) \right] \tag{4}$$

If the crack tip follows 3-membered rings, D_2, in hydrolysis with a much lower barrier, E_a (hydrolysis), then the slope of $\log V$ versus K_1 is less steep (Region I) and higher crack velocities are predicted for higher concentrations of water, as is observed experimentally [11].

In vitreous-silica

$$[D_2] < [D_1] \tag{5}$$

by a factor of at least 4 [12–14] and the prior AM1 MO models predict [2] that:

$$E_a(\text{hydrolysis}) \leqslant E_a(\text{ring contraction}).$$

With an increase in the concentration of 4-membered rings, $[D_1]$ in a-silica along with an increase in E_a (ring contraction), Region III should be steeper and occur at higher stress intensities, as is observed [11]. The difference in ring concentration, β_a, also explains why the slope of Region III crack growth is 3 to 4 times steeper than Region I.

It is well known that slow crack growth occurs below the ultimate fracture strength of a-silica [9]. This is classically explained by the existence of stress concentrations that eventually lead to bond breaking [9]. However, it is probable that a significant component of stress concentration involves ring contraction at energies "below" those required to break a Si–O bond [1,2]. The energy of contraction is consumed in distorting bond angles, as well as bond distances, from their lowest energy configurations, as summarized in Fig. 3 (based on [14]).

In this study, some models of the 5-fold and 6-fold ring contractions that lead to crack growth are predicted to have very low barriers to water-free fracture.

2. AM1 molecular orbital models

In this study we use AM1 molecular orbital theory [3,4] within the parameters of MOPAC 6.1 [5]. The strengths, limitations, and applications of the AM1 MO method have been discussed previously [1,15–17]. The Austin Method (AM1) [1,2] semi-empirical calculations reduce the problems encountered in analysing distorted structures by modifying the core repulsion function used in modified neglect of distance overlap (MNDO) methods with additional Gaussian terms and the calculated structures and heats of formation match quite well with experimental values [4,5,17].

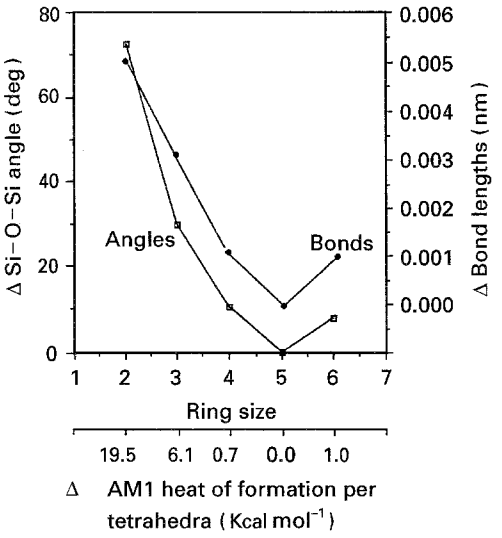

Figure 3 Differences in the AM1 models of silica ring bond angles and bond lengths.

In studying fracture, it is necessary to be aware of the limitations of the AM1 method. A model of simple Si–O bond breaking will not yield realistic results due to the creation of unpaired electrons in the reaction. AM1, and other semi-empirical methods, do not include the wavefunctions for unpaired electrons. This limitation is overcome by using *ab initio* generalized valence bond (GVB) theory. However, the GVB level of theory is difficult to apply to structures large enough to simulate a fracture process. Another limitation in the physics of the AM1 theory is that anti-bonding wavefunctions are ignored. During bond breaking anti-bonding wavefunctions may be important. Therefore, in previous studies [1, 2] the magnitude of this problem with AM1 was modelled using Restricted Hartree Fock (RHF), Unrestricted Hartree Fock (UHF) and Configuration Interaction (CI) methods within the parameters of MOPAC. It was found that UHF level of theory modelled the fracture process within acceptable limits.

In this study, all geometries and transition states were modelled using AM1, UHF, Precise theory within MOPAC 6.1. Some structures were optimized initially using RHF and were used as starting points for the UHF calculations.

3. Results for 5-fold ring fracture

Figs 4 through 9 show the results of fracture via various 5-fold silica ring contractions. The AM1 optimized 5-fold ring (Fig. 4) was strained across the ring. The initial Si–Si distance before the strain was applied was 0.52 nm. The transition state, or saddle, occurred at 0.55 nm (Fig. 5) with a barrier to fracture of + 8 Kcal mol^{-1}. This is a significantly lower barrier than the contraction of a 4-fold ring (65 Kcal mol^{-1}) [1]. The 5-fold ring contracted into a 4-fold ring by extracting a single silica tetrahedra (Fig. 6) with a Si–Si strain of 0.68 nm. The reverse reaction is usually called a "relaxation process" (via sintering) [18] and has a calculated barrier of + 7 Kcal mol^{-1}. Fig. 7 shows the change in heat of formation as a function of structure and strain in the Si–Si distance for the 5-fold silica ring. The RHF calculation has a barrier approximately twice that of UHF and is shown for comparison.

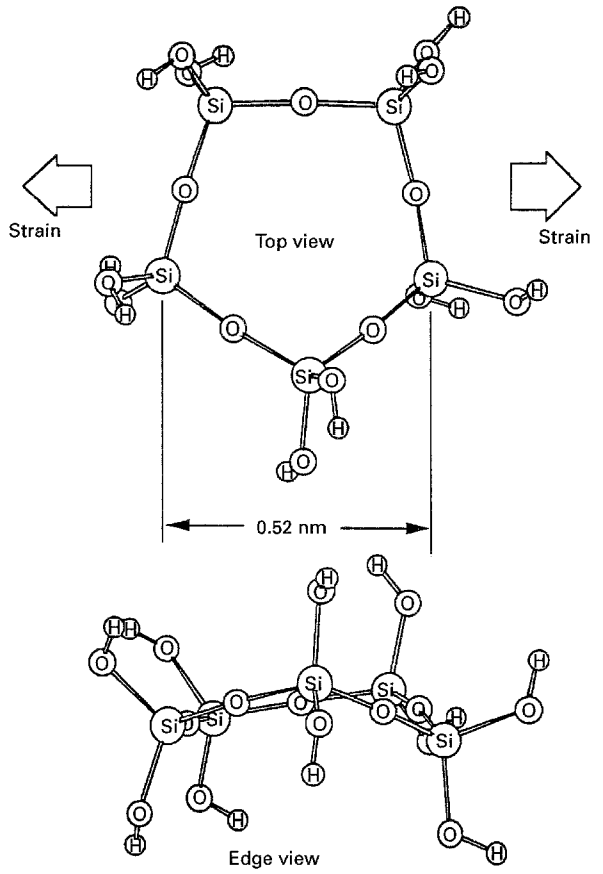

Figure 4 AM1 Model of cyclopentasiloxane: a 5-fold silica ring. AM1 heat of formation = − 1243 Kcal mol^{-1} (model R5).

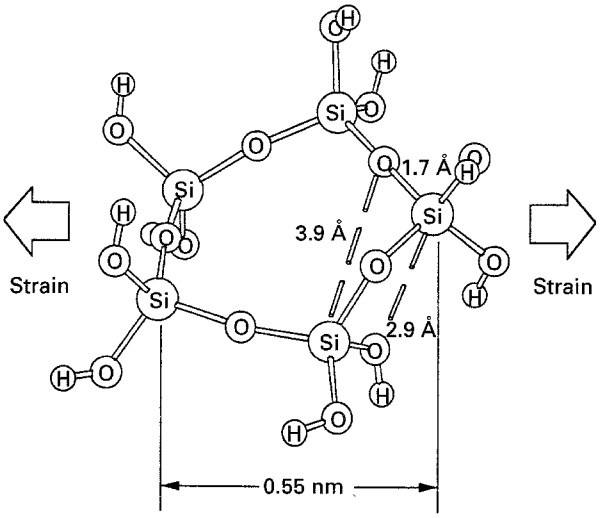

Figure 5 AM1 UHF transition state (saddle) for a 5-fold ring contraction into a 4-fold ring. UHF AM1 heat of formation = − 1235 Kcal mol^{-1} (model BB46). Fracture barrier = + 8 Kcal mol^{-1}. Sintering barrier = + 7 Kcal mol^{-1}.

Because of the larger ring size other contraction paths are also possible. Comparing Fig. 4 with Figs 8 and 9 shows two other possibilities. The 5-fold ring is able to contract into smaller rings such as a 3-fold ring and a 2-fold ring (Fig. 8) or a condensation reaction may occur between neighbouring silanols to form

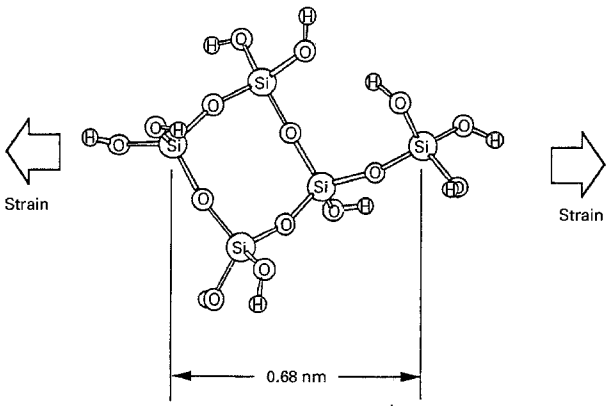

Figure 6 End point structure for a 5-fold to 4-fold ring contraction with the extraction of a silica tetrahedra. UHF AM1 heat of formation = -1242 Kcal mol^{-1} (model BB49).

a water molecule, as in Fig. 9. These each have barriers to fracture of $+20$ and $+52$ Kcal mol^{-1}, respectively.

4. Results for 6-fold ring fracture

Figs 10 through 14 show the results of fracture via various 6-fold ring contraction calculations. The initial 6-fold ring is shown in Fig. 10. It was strained

Figure 9 End product of a 5-fold ring contraction into two 3-fold rings while releasing a water molecule. UHF AM1 heat of formation = -1224 Kcal mol^{-1} (model BB63). Barrier to fracture = $+52$ Kcal mol^{-1}. Barrier to sintering = $+32$ Kcal mol^{-1} (model BB66).

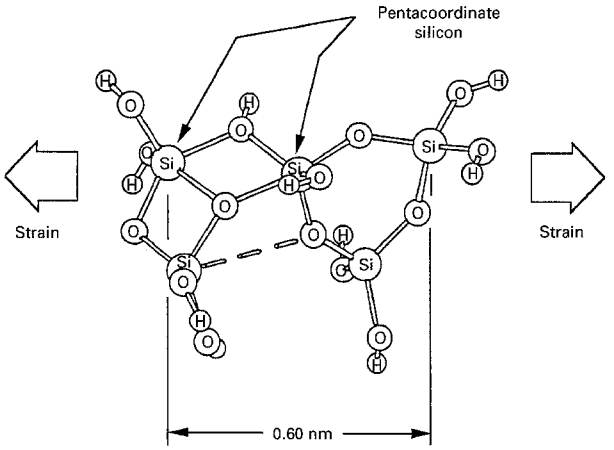

Figure 8 AM1 UHF transition state (saddle) for a 5-fold ring contraction into 3-fold and 2-fold rings. AM1 UHF heat of formation = -1223 Kcal mol^{-1} (model BB61). Barrier to fracture = $+20$ Kcal mol^{-1}. Barrier to sintering = $+6$ Kcal mol^{-1}.

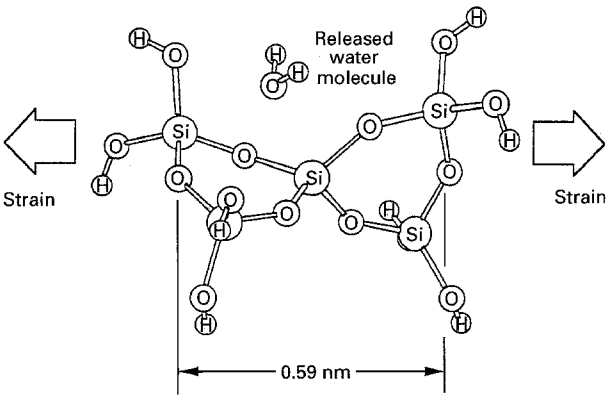

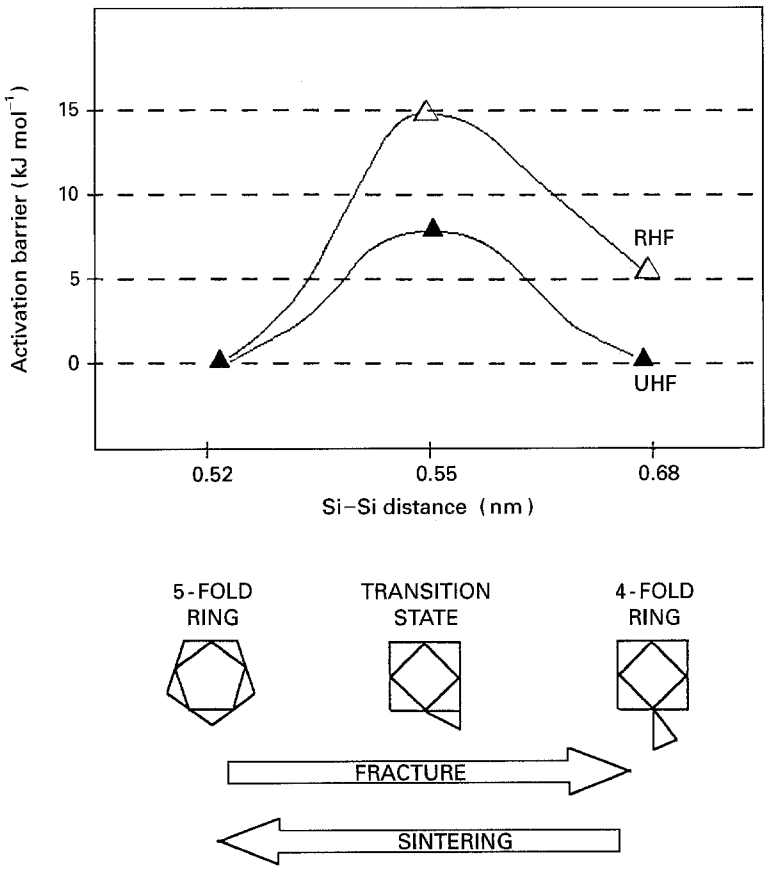

Figure 7 5-fold to 4-fold ring contraction barrier.

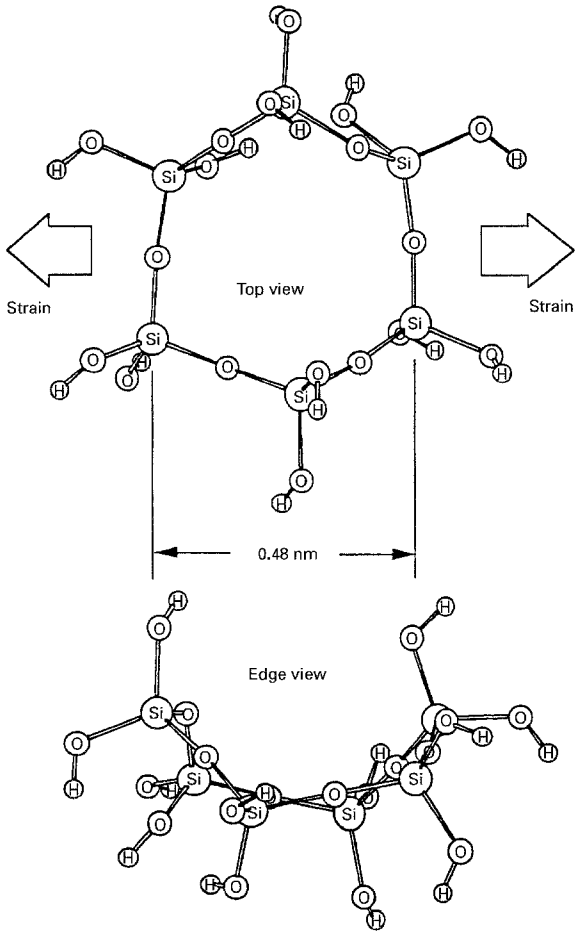

Figure 10 AM1 model of cyclohexasiloxane: a 6-fold silica ring. AM1 heat of formation = − 1485 Kcal mol^{-1} (model R6).

across the ring as was the 5-fold structure. Fig. 11 shows that the transition state (saddle point) occurs at a Si–Si strain of 0.75 nm with a barrier to fracture of + 41 Kcal mol^{-1}. The barrier to sintering or relaxation is + 39 Kcal mol^{-1}. The end point of this ring contraction, with an extracted silica tetrahedra, is shown in Fig. 12.

Fig. 13 shows an alternative reaction transition state for 6-fold ring contraction into two 4-fold rings via a condensation reaction of two silanols to form a water molecule. This barrier to fracture was unexpectedly small at only + 9 Kcal mol^{-1}. The barrier to sintering was larger at + 22 Kcal mol^{-1}. This structure was initially discovered by Allinger and coworker [19, 20] using a molecular mechanics (MM2) reaction coordinate calculation. Our reaction path calculation shows that the 6-fold ring elongates easily under strain and silanols appear to interact. AM1 was used to identify that a condensation reaction was structurally possible, leading to the final structure of two 4-fold rings as shown in Fig. 14, at a Si–Si strain of 0.68 nm.

5. Conclusion

Fig. 15 summarizes the various fracture paths of a-silica via ring contraction found in this study. Extraction of a single tetrahedra is more easily accomplished with a 5-fold ring than for a 6-fold ring. Conversely, the formation of a water molecule at the crack tip, from strain-induced condensation of structural silanols, seems easier with a 6-fold ring than for a 5-fold ring.

The possibility of forming a water molecule during water-free fracture of a-silica with structural silanols on non-bridging oxygens is an interesting finding. With water available, hydrolysis of neighbouring ring structures is possible which considerably lowers the barrier to fracture. This may cause "self induced hydrolysis" at the crack tip as postulated in Fig. 15.

A large number of reaction pathways to fracture are still unexplored for 4-fold, 5-fold, 6-fold, and larger-membered silica rings. However, these results indicate

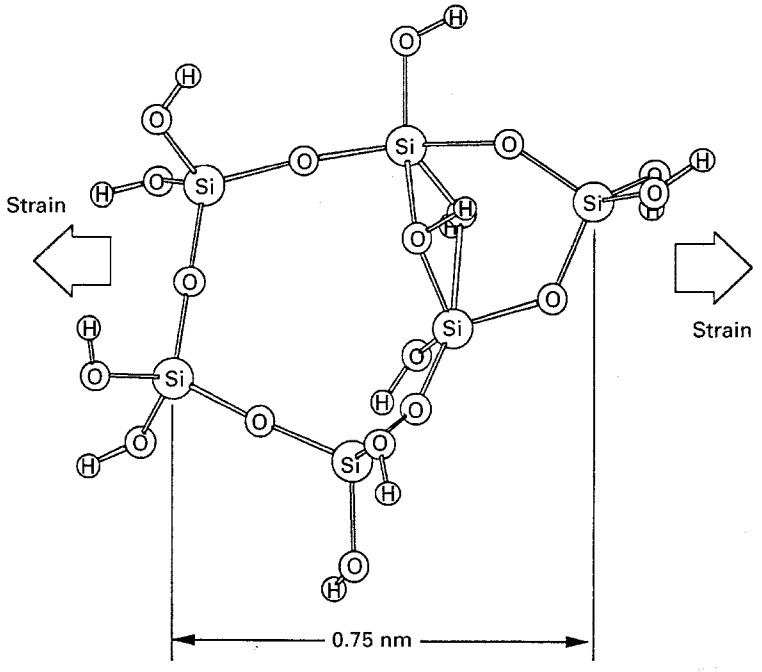

Figure 11 AM UHF transition state (saddle) for a 6-fold ring contraction into a 5-fold ring. UHF AM1 heat of formation = − 1445 Kcal mol^{-1} (model BB65). Barrier to fracture = + 41 Kcal mol^{-1}. Barrier to sintering = + 39 Kcal mol^{-1}.

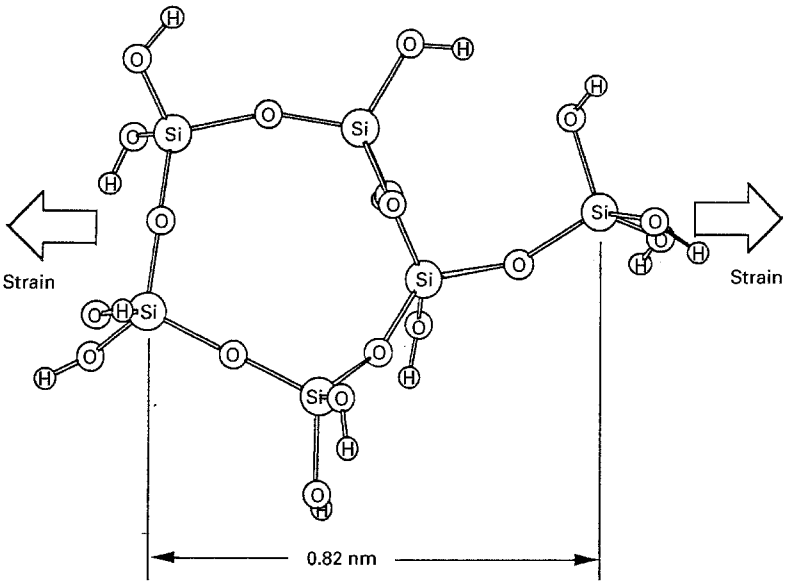

Figure 12 End point of a 6-fold ring contraction into a 5-fold ring. AM1 heat of formation = $-1483\ \text{Kcal mol}^{-1}$ (model BB64).

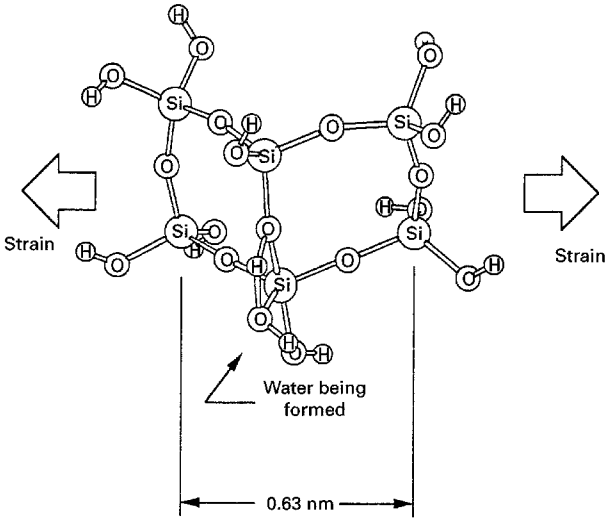

Figure 13 AM1 UHF transition state (saddle) for a 6-fold ring contraction into two 4-fold rings while forming a water molecule. UHF and RHF AM1 heat of formation = $-1476\ \text{Kcal mol}^{-1}$ (model BB53). Barrier to fracture = $+9\ \text{Kcal mol}^{-1}$. Barrier to sintering = $+22\ \text{Kcal mol}^{-1}$.

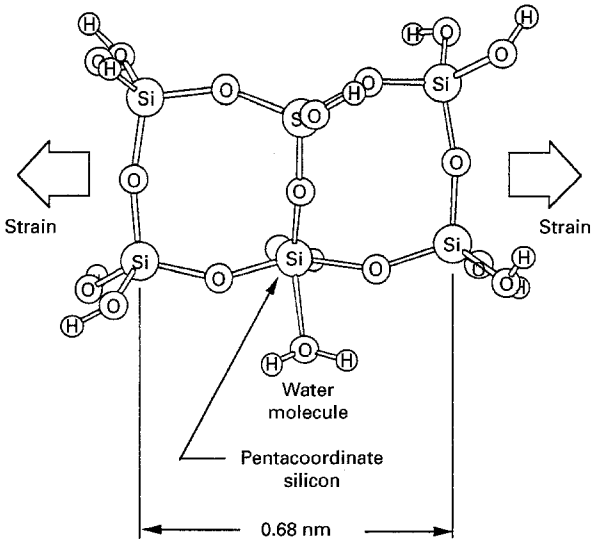

Figure 14 End point of a 6-fold ring contraction into two 4-fold rings and the release of a water molecule. UHF AM1 heat of formation = $-1224\ \text{Kcal mol}^{-1}$ (model BB52).

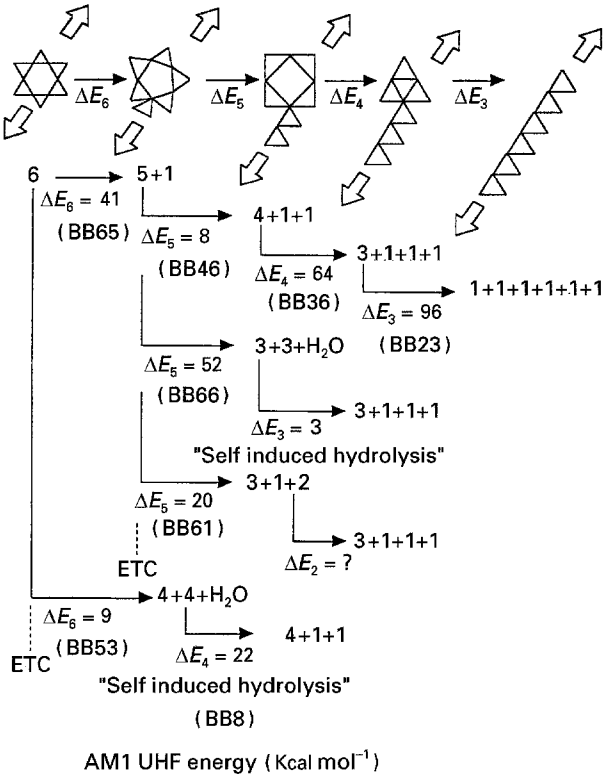

Figure 15 Schematic of various ring contraction schemes that could occur during slow crack growth.

that large rings will generally break via ring contraction whereas small rings will open via hydrolysis if water is available as the crack tip seeks out the lowest energy pathway for slow crack growth. Thus, the transition from Region I to Region II crack growth is a function of the local distribution of silica ring sizes in a-SiO_2 as well as related to relative humidity of the fracture environment.

Acknowledgements

The authors gratefully acknowledge the support of the Air Force Office of Scientific Research, (Grant No.

F49620-92-J-0351). We also acknowledge the help and support of CAChe Scientific, Inc., Beaverton, OR.

References

1. J. K. WEST and L. L. HENCH, *J. Mater. Sci.* **29** (1994) 3601.
2. *Idem, ibid.* **29** (1994) 5808.
3. M. J. S. DEWAR, E. G. ZOEBISCH, E. F. HEALY and J. P. STEWART, *J. Amer. Chem. Soc.* **107** (1985) 3902.
4. M. J. S. DEWAR and C. JIE, *ibid.* **6** (1987) 1486.
5. MOPAC Version 6.1, Tektronix Inc., CaChe Scientific, Beaverton, OR.
6. J. K. WEST and S. WALLACE, in "Chemical Processing of Advanced Materials", edited by L. L. Hench and J. K. West (John Wiley and Sons, New York, 1992) p. 159.
7. S. WALLACE, J. K. WEST and L. L. HENCH, *J. Non-Cryst. Solids* **152** (1993) 101.
8. J. K. WEST and S. WALLACE, *ibid.* **152** (1993) 109.
9. S. W. FREIMAN, in "Glass Science and Technology, Vol. 5 Elasticity and Strength in Glass", edited by D. R. Uhlmann and N. J. Kreidl (Academic Press, New York, 1980) pp. 21–79.
10. T. A. MICHALSKE and B. C. BUNKER, *J. Appl. Phys.* **56** (1984) 2686.
11. S. M. WIEDERHORN, *J. Amer. Ceram. Soc.* **50** (1967) 407.
12. F. L. GALEENER, *J. Non-Cryst. Solids* **49** (1982) 53.
13. J. K. WEST and L. L. HENCH, *J. Amer. Ceram. Soc.* **78** (4) (1995) 1093.
14. *Idem, J. Non-Cryst. Solids* **180** (1994) 11.
15. L. P. DAVIS and L. W. BURGGRAF, in "Ultrastructure Processing of Advanced Ceramics", edited by J. D. Mackenzie and D. R. Ulrich (Wiley, New York, 1988) p. 367.
16. L. W. BURGGRAF, L. P. DAVIS and M. S. GORDON, in "Ultrastructure Processing of Advanced Materials", edited by D. R. Uhlmann and D. R. Ulrich (Wiley, New York, 1992) p. 47.
17. J. J. P. STEWART, *J. Computational Chem.* **50** (1989) 221.
18. C. J. BRINKER and G. W. SCHERER, "Sol–Gel Science" (Academic Press, New York, 1990).
19. N. L. ALLINGER, *J. Amer. Chem. Soc.* **99** (1977) 8127.
20. U. BURKERT and N. L. ALLINGER, "Molecular Mechanics" (American Chemical Society, Washington, DC, 1982).

Received 8 September 1994
and accepted 22 June 1995